Nucleic Acids Research, 2001, Vol. 29, No. 15 **3145–3153**

Bulged residues promote the progression of a loop–loop interaction to a stable and inhibitory antisense–target RNA complex

Fabrice A. Kolb, Eric Westhof, Chantal Ehresmann, Bernard Ehresmann, E. Gerhart H. Wagner[1] and Pascale Romby*

UPR 9002 du CNRS, Institut de Biologie Moléculaire et Cellulaire, 15 rue Rene Descartes, 67084 Strasbourg Cedex, France and [1]Institute of Cell and Molecular Biology, Biomedical Center, Uppsala University, Box 596, Husargatan 3, S-75124 Uppsala, Sweden

Received May 8, 2001; Revised and Accepted June 20, 2001

ABSTRACT

In several groups of bacterial plasmids, antisense RNAs regulate copy number through inhibition of replication initiator protein synthesis. These RNAs are characterized by a long hairpin structure interrupted by several unpaired residues or bulged loops. In plasmid R1, the inhibitory complex between the antisense RNA (CopA) and its target mRNA (CopT) is characterized by a four-way junction structure and a side-by-side helical alignment. This topology facilitates the formation of a stabilizer intermolecular helix between distal regions of both RNAs, essential for *in vivo* control. The bulged residues in CopA/CopT were shown to be required for high *in vitro* binding rate and *in vivo* activity. This study addresses the question of why removal of bulged nucleotides blocks stable complex formation. Structure mapping, modification interference, and molecular modeling of bulged-less mutant CopA–CopT complexes suggests that, subsequent to loop–loop contact, helix propagation is prevented. Instead, a fully base paired loop–loop interaction is formed, inducing a continuous stacking of three helices. Consequently, the stabilizer helix cannot be formed, and stable complex formation is blocked. In contrast to the four-way junction topology, the loop–loop interaction alone failed to prevent ribosome binding at its loading site and, thus, inhibition of RepA translation was alleviated.

INTRODUCTION

Many antisense RNAs are regulators of plasmid copy number (1). Plasmid R1 belongs to the IncFII family of plasmids which shares the overall genetic organization with respect to replication control functions. In plasmid R1, replication is negatively controlled at the translational level by binding of the antisense RNA (CopA) to its target site (CopT) in the leader region of the *repA* mRNA, ~80 nt upstream of the *repA* start codon (2). Synthesis of the replication initiator protein RepA requires translation of a short leader peptide (*tap*), encoded upstream of *repA*. Binding of CopA prevents *tap* translation by occluding ribosome binding at the *tap* ribosome binding site (RBS), and thereby *repA* expression is inhibited (3–5). Interestingly, several copy number control antisense RNAs which all inhibit translation of replication initiator proteins have structural properties similar to those of CopA. These RNAs are fully complementary to their target site and contain a long stem–loop structure. For proper control, the intracellular concentration of the antisense RNA must be a measure of the plasmid concentration: this is ensured by constitutive synthesis and a short half-life of these RNAs (6). Furthermore, efficiency of *in vivo* control is correlated with high rates of antisense RNA binding to its target site [in the order of 10^6 $M^{-1}s^{-1}$ (7)]. This class of antisense RNAs does not require *trans*-acting proteins to promote inhibition. Thus it can be speculated that the structure of these antisense RNAs has evolved to be optimized for the critical steps that determine their regulatory functions.

Kinetic studies have shown that the initial step of antisense RNA binding involves a loop–loop interaction mediated by a limited number of Watson–Crick base pairs, the so-called kissing complex [R1 (8); pMU720 (9); ColIb-P9 (10,11)]. In plasmid R1, we have recently shown that this loop–loop interaction is rapidly converted into a stable and inhibitory complex formed through a hierarchy of distinguishable intermediates, and that the formation of a full duplex *in vitro* is too slow to be of biological relevance (12–14). The major product of the binding reaction adopts an unusual structure characterized by a four-helix junction. Its formation involves extensive breakage of intramolecular base pairs to promote the formation of two intermolecular helices (see Fig. 1) (13). This conversion is essential for the formation of an irreversible complex and for the activity of the antisense RNA *in vivo* (14). We proposed previously that the four-way junction structure could promote a side-by-side helical alignment to allow formation of a third long intermolecular helix, involving the 5′ tail of CopA and the complementary region of CopT (13). Recent data indicated that a topology, strikingly similar to that of the stable CopA–CopT complex, may be present in complexes of all R1-related plasmids (11,15). This structure completely and irreversibly

*To whom correspondence should be addressed. Tel: +33 3 88 41 70 51; Fax: +33 3 88 60 22 18; Email: p.romby@ibmc.u-strasbg.fr

inhibits *repA* translation, mainly by occluding ribosome binding [e.g. pMU720 (16); R1 (5); Col1b-P9 (17)].

In addition to the recognition loops and the single-stranded regions required for stable complex formation, these antisense and target RNAs carry internal loops or unpaired residues in the major stem close to the hairpin loop. This is characteristic for antisense RNAs with long hairpins for which, unlike RNAI/RNAII of ColE1 (18,19), no protein is involved in regulation. The upper stem structure-disrupting elements can have several functional implications. They protect the RNAs against the double strand-specific RNase III since removal of bulged residues rendered CopA sensitive to cleavage *in vivo* and *in vitro* (20). Furthermore, their deletion strongly affected control *in vivo* and rapid formation of stable antisense/target RNA complexes *in vitro* [R1 (21); pUM720 (22); Col1b-P9 (23)]. Importantly, the positioning of these bulged residues close to the apical loop is critical since an internal loop placed at the bottom part of the stem did not restore inhibitory activity (21).

In the present paper, we show that removal of the bulged residues in CopA and CopT interferes with progression of the initial loop–loop helix towards the four-way junction. Instead, the loop–loop interaction formed by bulge-less CopA and CopT complex becomes arrested in a state that involves pairing of all loop bases, and does not convert to a stable complex. This complex fails to prevent ribosome binding at *tap* RBS.

MATERIALS AND METHODS

Oligodeoxyribonucleotides

Oligodeoxyribonucleotides were bought from IBA-NAPS. Primers for the generation of transcription templates were for $CopT_{302}$: T7GG, 5′-GAA ATT AAT ACG ACT CAC TAT AGG TTA AGG AAT TTT GTG GCT GG-3′ (T7 RNA polymerase promoter sequence underlined) and SeqP/II, 5′-CGG ATT CGG GTT CTT TA-3′; for $CopT_{74}$: GW46, 5′-GAA ATT AAT ACG ACT CAC TAT AGG CCC CGA TAA TCT TCT TCA ACT T-3′ and GW47, 5′-TGT TGG CTA TAC GGT TTA AGT-3′; for CopA: T7-SA, 5′-GAA ATT AAT ACG ACT CAC TAT AGT AGC TGA ATT GTT GGC TAT ACG-3′ and T7-EA, 5′-AAA GCA AAA ACC CCG ATA ATC TTC-3′. The primers for CopI were T7-SI, 5′-GAA ATT AAT ACG ACT CAC TAT AGG GCC CCG GTA ATC TTT TCG T-3′ and T7-EI, 5′-AAA CCC CGA TAA TCT TCT TCA-3′. SeqP/II was also used for primer extension in the toeprinting experiments.

DNA templates and RNA synthesis

CopT, CopA, CopI and mutant RNAs (Lo, Up, L/U) were synthesized by T7 RNA polymerase from PCR-generated DNA fragments as described (20). PCR fragments were generated from plasmid pGW58 carrying the wild-type *copA/copT* region (3), and from mutant plasmids (20). Transcription of CopT yields a run-off product of 302 nt initiated with GG instead of the GU sequence of the wild-type *repA* mRNA. A shorter $CopT_{74}$ corresponding to the complementary sequence of the antisense RNA was also produced, the RNA starts with GG instead of AG, i.e. CopA RNA contains a 5′ terminal G instead of an A residue. Neither of these nucleotide changes affects structure or binding properties. CopA and CopI mutants contained either a U52-A64:2 base pair inserted in the upper stem (Lo), or a C47:2-G69 base pair instead of a bulged guanine 69 (Up), or both (L/U) (Fig. 1) (20). The complementary changes were also introduced in CopT mutants. RNAs were purified from 8% polyacrylamide–urea gels.

5′ End-labeling of dephosphorylated RNA was performed with T4 polynucleotide kinase and [γ-^{32}P]ATP (24). Labeled RNAs were purified by polyacrylamide–urea gel electrophoresis, eluted and precipitated twice with ethanol. Before use, the RNAs were dissolved in water and renatured by incubation at 90°C for 2 min, followed by slow cooling at 20°C in TMN buffer (20 mM Tris-acetate pH 7.5, 10 mM Mg-acetate, 100 mM sodium acetate).

Enzymatic and chemical probing

Antisense RNA binding was carried out at 37°C for 15 min in TMN buffer with end-labeled CopT (3×10^{-8} M) and a 5-fold excess of unlabeled CopA or CopI (1.5×10^{-7} M), or with end-labeled CopA or CopI (4×10^{-8} M) and a 5-fold excess of unlabeled CopT (2×10^{-7} M). Full duplexes between CopT and CopA species were formed by incubation at 90°C for 2 min followed by slow cooling to 37°C in TMN buffer. RNase V1 hydrolysis, Pb^{2+}-induced hydrolysis and modification [N7]G by lead- and nickel-complex (NiCR) were done as previously described (13). Cleavage positions were identified by running, in parallel, RNase T1, RNase U2 and alkaline ladders of the end-labeled RNA (25). Incubation controls were done to detect nicks in the RNA.

Phosphate modification interference with ethylnitrosourea

5′ End-labeled RNA (10 nM) was first modified in 50 µl of buffer containing 50 mM sodium cacodylate pH 8.0, 1 mM EDTA with 16 µl of an ethylnitrosourea (ENU)-saturated ethanol solution for 1 min at 90°C. Reactions were stopped by ethanol precipitation with 0.3 M sodium acetate. Pellets were dissolved in TMN buffer, and complexes were formed with 1–5 nM of the unlabeled complementary RNA. An aliquot of labeled RNA was submitted to the same treatment except that ENU was omitted. Free and complexed RNAs were separated by electrophoresis at 4°C on 8% non-denaturing polyacrylamide gels in 45 mM Tris-borate pH 8.3. The corresponding bands were identified by autoradiography, cut out, and the RNA was eluted overnight at 4°C in 500 mM ammonium acetate pH 6, 0.1 mM EDTA, followed by precipitation. Ethylated phosphates were identified by incubating the modified RNA in 10 µl of 0.1 M Tris–HCl pH 9.0 at 50°C for 10 min. The control experiment was submitted to the same treatment. After precipitation, the RNA fragments were separated by denaturing gel electrophoresis on 15% polyacrylamide gels. Cleavage positions were identified by running in parallel RNase T1, and alkaline ladders of the end-labeled RNA.

Toeprinting assays

Toeprinting was performed essentially as previously described (5). The [^{32}P]5′ end-labeled primer SepP/II was first annealed to CopT RNA in 20 mM Tris-acetate pH 7.5, 60 mM NH_4Cl, 3 mM β-mercaptoethanol, heated at 90°C for 1 min and cooled on ice for 1 min. After the addition of 10 mM Mg-acetate, the RNA was incubated at 20°C for 20 min. Initiation complex formation was performed at 37°C from 30 s to 15 min in a reaction mixture containing 10 mM Tris-acetate pH 7.4, 60 mM

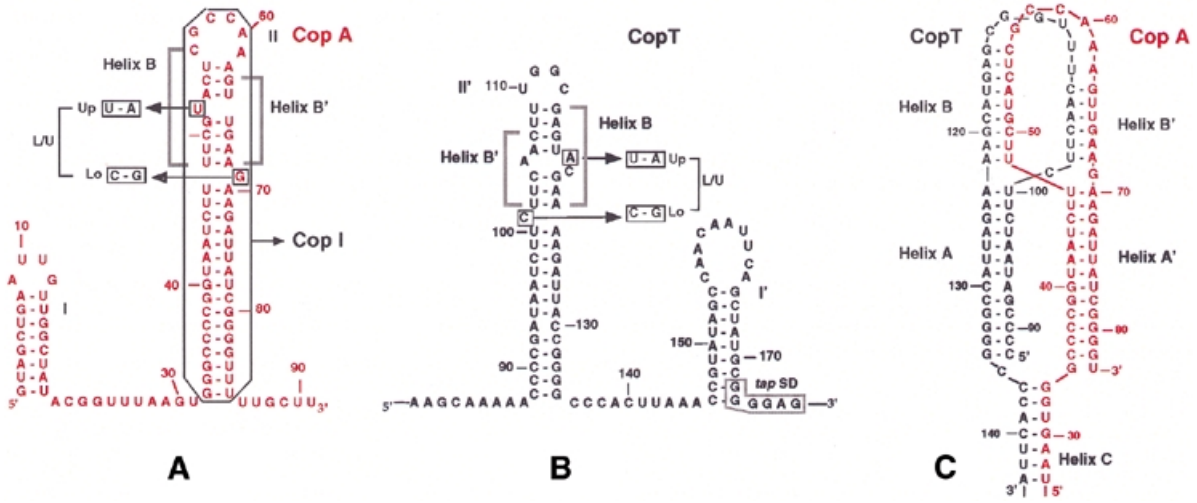

Figure 1. Secondary structures of the antisense RNA CopA (**A**), its target site CopT (**B**) and the stable CopA–CopT complex (**C**). The sequence of CopI is framed. Positions of mutations Lo, Up and L/U are shown on both RNAs. The Shine–Dalgarno sequence at *tap* is indicated. The secondary structure model for CopA–CopT is from Kolb *et al.* (13).

NH_4Cl, 10 mM Mg-acetate, 6 mM β-mercaptoethanol and, unless otherwise stated, 40 nM CopT RNA, 125 nM 30S subunits and 1 μM $tRNA_f^{Met}$. In the toeprinting inhibition experiments, antisense RNA/target RNA complexes were formed prior to ternary complex formation at 37°C for 15 min (as described above) in the presence of a 5-fold excess of CopA or CopI species, followed by the addition of 30S and tRNA. Concentrations of the antisense RNA was chosen to get an optimal formation of the kissing complex. Primer extension reactions were subsequently performed at 37°C for 15 min by adding 2 U of AMV reverse transcriptase (Life Sciences). Reactions were stopped by phenol extraction and ethanol precipitation.

Graphic modeling

The 3D model of CopT-L/U (nucleotides C88 to A178) interacting with CopA-L/U (nucleotides G1 to U87) was built using several algorithms (26) incorporated in the program MANIP (27). The generated model was subjected to restrained least-squares refinement using the programs NUCLIN and NUCLSQ (26) in order to ensure geometry and stereochemistry with allowed distances between interacting atoms and to avoid steric conflicts. The color views were generated with the program DRAWNA (28).

RESULTS

The loop–loop interaction is essential to initiate pairing in the wild-type and mutant complexes

Mutations in CopA and CopT which generated fully helical upper stems decreased the rate and stability of stable CopA–CopT complex formation by more than one order of magnitude (21). These effects suggested the topology of mutant and wild-type complexes to be different. Here, we used chemical modification interference experiments to probe the initial interaction in the wild-type CopA–CopT, CopI–CopT and mutant CopI-L/U–CopT-L/U complexes. CopI is a truncated CopA, unable to form the stable complex with CopT, but capable of forming the extended kissing complex (8,13). In the L/U mutant RNAs, the bulged nucleotides have been replaced by standard Watson–Crick base pairs (Fig. 1) (20,21). Phosphate groups were modified by treatment with *N*-ethyl-*N*-nitrosourea. The protocol used ensured ethylation of the non-bridging oxygens to, on average, less than one modification per molecule. Such an approach had been successfully used to probe the loop–loop interaction involved in the dimerization process of HIV-1 RNA (29). Modified antisense or target RNAs were allowed to form complexes with their counterparts. Free RNA and RNA–RNA complex, were separated by gel electrophoresis under native conditions and eluted from the gel. Sites of modifications in each fraction were then identified by alkaline treatment which induces RNA scission at the modified phosphate. Cleavages present in the free RNA species but absent from the ones in the complex indicate the positions at which modification prevents complex formation (negative interference). Consequently, the free RNA fraction is enriched for RNA species that carry modifications that interfere with complex formation, and thus the cleavages corresponding to the positions of negative interference are enhanced (Fig. 2, lanes F).

Strong inhibition of wild-type CopA–CopT complex formation was observed upon ethylation of phosphates 112–114 in CopT, and 58–59 in CopA (Fig. 2A and B). Interestingly, the strongest interference pinpointed a subset of nucleotides in both CopT and CopA loops (Fig. 2D) in which many copy number mutations had been mapped [5′-GGCG in CopT; e.g. (30)]. In addition, ethylation of phosphates 111, 115–120 in CopT, and phosphates 57 and 60 in CopA, resulted in partial interference. Identical results were obtained with the truncated antisense RNA, CopI (result not shown). The mutant complex formed between CopI-L/U and CopT-L/U was also analyzed (Fig. 2C). Compared to the wild-type case, a single and extended region of strong negative interference was observed, comprising phosphates 57–62 within the loop of CopI-L/U (Fig. 2D). In addition, partial interference was observed upon modification of phosphates 54–56 in the 5′ part of the CopI-L/U stem. Given the number of modifications that prevent complex

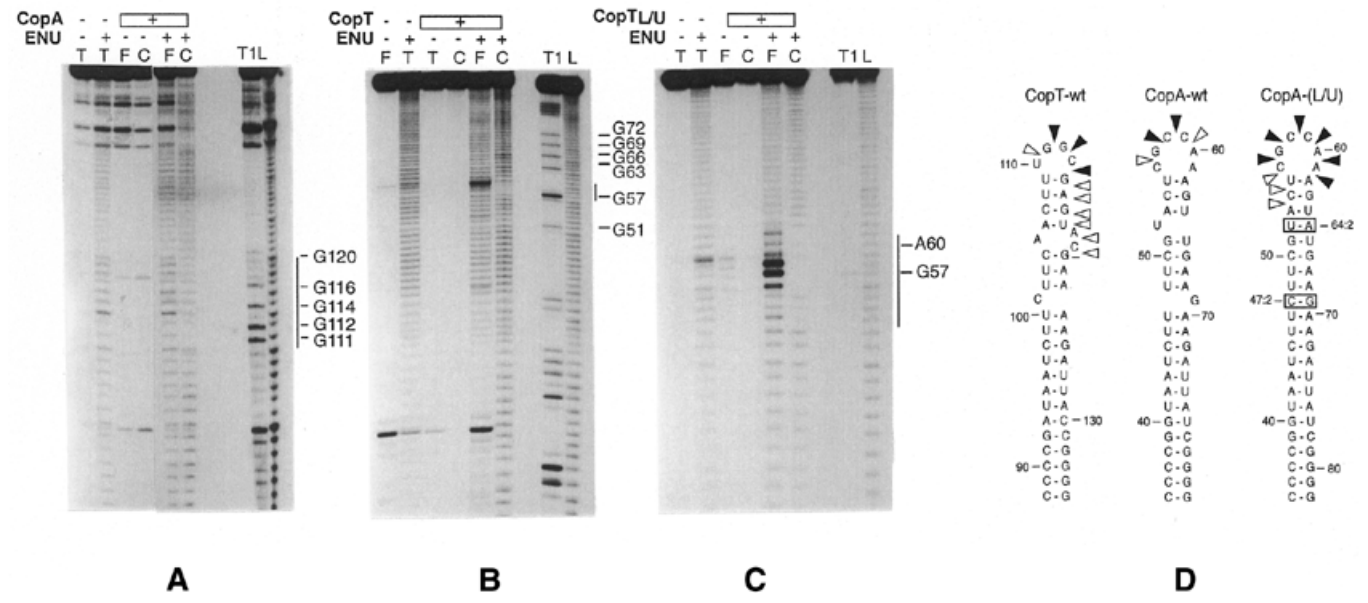

Figure 2. Effect of phosphate ethylation on complex formation. 5′ End-labeled CopT (**A**), CopA (**B**) and CopI-L/U (**C**) were modified with ENU and submitted to complex formation with either CopA (A), CopT (B) and CopT-L/U (C). F and C refer to RNA extracted from the bands containing the free RNA and the RNA–RNA complex, respectively; T corresponds to the total population of unmodified and ENU-modified CopA used for the interference experiment. (+) and (–) RNA are treated or untreated with ENU, respectively. Lanes T1 and L correspond to RNase T1 and alkaline ladders. Negative interference is indicated by vertical bars on the autoradiograms. In (B), lanes F, the cleavage at position U27 found in the free RNA population is not specific and may originate from a fortuitous RNase contamination. (**D**) Secondary structures of the RNAs showing the position of modified phosphates which interfere with complex formation. Filled and empty triangles indicate strong and weak interference, respectively. For clarity, the numbering of nucleotides in CopI-L/U was identical to that of wild-type CopI, except that the additional nucleotides were assigned as positions 47:2 and 62:2. Mutations are boxed.

formation, this negative interference may also reflect local perturbation of the CopA/I and CopT loop structures.

These experiments indicate that, in both the wild-type and L/U mutant cases, modification of phosphates within the recognition loops interfered with complex formation. This suggests that removal of bulges did not impair formation of the initial loop–loop interaction. However, the differences in the interference patterns observed between the wild-type and mutant complex suggest that these two complexes adopt different topologies.

Removal of the bulged residues prevents the formation of the intermolecular helices

We previously showed that the initial loop–loop interaction is converted to an unusual four-way junction structure (13). The initial base pairs formed are disrupted to permit helix progression into the upper stems, resulting in the formation of two intermolecular helices B and B′ (Fig. 1C). RNase V1 probing of CopA–CopT or CopI–CopT complexes provided a characteristic signature for helices B and B′ (Fig. 3A) (13): new or enhanced cleavages were induced in CopA or CopI at consecutive positions U52–C56 (helix B), and in CopT at C104–A105 (helix B′). In addition, the intermolecular helix C, which greatly enhances CopA–CopT complex stability, was characterized by the occurrence of several V1 cuts in the 3′ end of CopT, as well as by the disappearance of V1 cleavages in CopA at positions G7–A9 and G16–A19, resulting from melting of helix I (Fig. 3A). Thus, RNase V1 was used to probe the structure of the homologous antisense/target RNA complexes containing mutations of either the lower bulge (Lo), upper bulge (Up) or both (L/U) (Fig. 3B–D), as well as the heterologous complexes formed by wild-type CopA and mutant CopT RNAs (results not shown).

None of the mutant complexes presented the characteristic RNase V1 pattern observed for the wild-type complex. In the three homologous mutant complexes (CopA-Up/CopT-Up, CopA-Lo/CopT-Lo, CopA-L/U/CopT-L/U), helix C did not form properly. This is indicated by cleavages at positions 7–9 and 17–19 in CopA-Lo and CopA-L/U bound to their target CopT, which remained unchanged as compared to free mutant CopA (Fig. 3B and D), whereas CopT-Up induced only weak protections at positions 17–19 in CopA-Up (Fig. 3C). Several new cuts were detected in the hairpin loops of CopA-Up (C54–C56), of CopA-Lo (U55 and C56) and of CopA-L/U (U55–C56, A60 and A61) upon binding of CopT-Up, CopT-Lo and CopT-L/U, respectively (Fig. 3). In addition, enhanced cleavages were observed on the 5′ side of the major stem of CopA-Lo and CopA-L/U. Conversely, in all three homologous mutant complexes, binding of CopA variant did not change the pattern of RNase V1 cleavage in the corresponding CopT target. In particular, no enhanced cleavages at C104–A105 were detected in mutant CopT, indicating that helix B′ is not formed in the mutant complexes (results not shown).

Thus, replacing the bulged residues by Watson–Crick base pairs in the antisense and target RNAs induced dramatic changes in the overall topology of the CopA–CopT complex: the two intermolecular helices B and B′ were not formed, and thus formation of the third intermolecular helix C could not occur. These data are in good agreement with the dramatic effects of these three mutations on the rate of stable CopA–CopT complex formation (21).

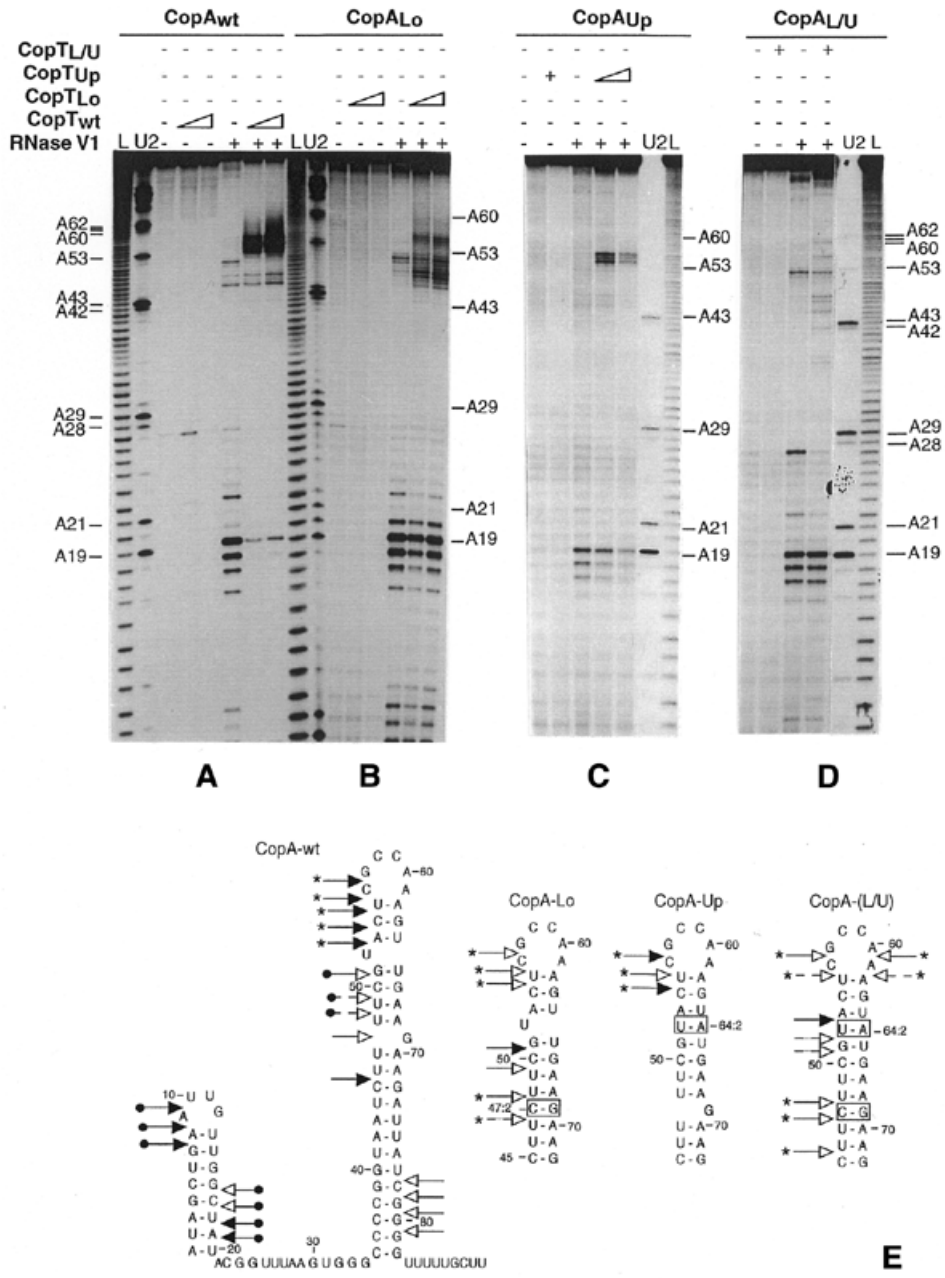

Figure 3. RNase V1 probing of homologous wild-type and mutated CopA–CopT complexes. Enzymatic hydrolysis was performed on 5′ end-labeled CopA-wt (**A**), CopA-Lo (**B**), CopA-Up (**C**) and CopA-L/U (**D**). Reactions were done in the absence or in the presence of an excess of wild-type or mutant CopT. Lanes U2 and L are RNase U2 and alkaline ladders, respectively. (**E**) Cleavages are shown on the secondary structure of the wild-type and mutant CopA by arrows. Only part of the secondary structure of the three mutant CopA, where changes induced by complementary CopT binding occurred, are shown. Effect of homologous CopT binding is as follows: asterisks, enhanced or new cut; filled circles, protection.

A fully base paired loop–loop interaction in the mutant CopA–CopT complexes

To obtain more detailed information on the accessibility of nucleotides within the CopA-L/U/CopT-L/U complex, NiCR-induced hydrolysis was used (13). Lead-induced cleavages occur mainly in single-stranded regions and in helices of low stability. NiCR modifies [N7]G and is very sensitive to stacking of base rings. Thus, N7 of purines within a helix are not reactive unless the deep groove is widened (31).

We showed previously that Pb^{2+}-cleavages in the CopA–CopT complex were restricted to unpaired residues located in the loops (C58–A61) connecting the two intermolecular helices B and B′ (13). In free CopA-L/U RNA, lead cleaved mainly in the hairpin loop and in the 5′ single-stranded region of the RNA (Fig. 4) (21). Binding of either CopT-L/U or CopT-wt induced strong protections at residues U55–A61 in the apical loop whereas minor protections were detected in the 5′ domain of CopA-L/U (Fig. 4A). This is supported by the NiCR probing experiment (Fig. 4B). In the major stem–loop of CopA-L/U, only the N7 position of G57 was modified whereas all guanines within the stem were unreactive. Notably, G69 which is base paired in CopA-L/U was not modified, whereas

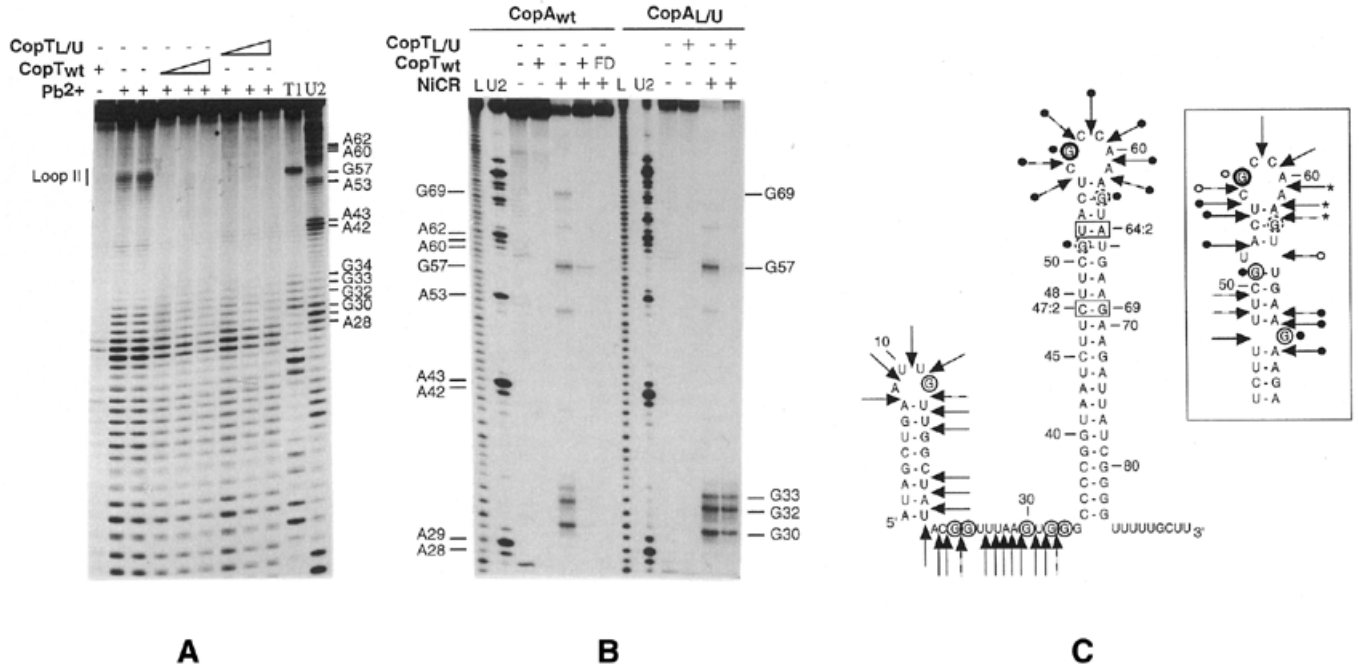

Figure 4. Chemical probing of CopA-L/U, free or in complex with CopT-L/U. (**A**) Pb^{2+}-induced hydrolysis was performed on 5′ end-labeled CopA-L/U alone (–) or in the presence of an excess of CopT-L/U or CopT-wt (+). Complex formation was performed at 37°C for 1, 5 and 10 min in TMN buffer. Lanes L, U2 and T1 are alkaline, RNase U2 and RNase T1 ladders, respectively. (**B**) NiCR modification on 5′ end-labeled CopA-wt or CopA-L/U: free (–CopT), bound to wild-type or mutant CopT under native conditions (+CopT/CopT-L/U). Full duplex with CopA (FD) was formed by denaturation/annealing treatment. (**C**) Secondary structure of CopA-L/U: G(N7) which are reactive under native conditions towards NiCR are circled, the line width of the symbols is proportional to the intensity of cleavage (strong, medium or weak). Pb^{2+}-cleavages are shown by arrows, dotted and full lines represent weak and moderate cleavages, respectively. Effect of CopT-L/U binding: strong and medium protections are shown by filled and empty circles, respectively; asterisks show enhanced cleavages. For comparison, the data obtained on CopA-wt bound to CopT-wt is shown in the insert.

it was reactive in CopA-wt (Fig. 4B). The only change induced by binding of CopT-L/U was restricted to the complete protection of G57 at N7 in CopA-L/U (Fig. 4B). In agreement with results from the RNase V1 probing, the stabilizer helix C was not formed in the CopA-L/U/CopT-L/U complex since position N7 of guanines 12, 23–24, 30, 32–33 in the 5′ domain of CopA-L/U were still reactive in the complex (Fig. 4B). Binding of CopT-Up also induced protection restricted to G57 at N7 in CopA-Up whereas G69 at N7 remained reactive towards NiCR (data not shown). By contrast, most of the N7 positions of guanines, with the notable exception of G57, showed protection towards NiCR in CopA-wt when bound to CopT-wt (Fig. 4B). In full duplexes (formed artificially), all the guanines at N7 of CopA-wt were fully protected by binding of CopT (Fig. 4B). Thus, these experiments allow us to distinguish between the full duplex, the extended kissing in CopA–CopT complex, and the loop–loop interaction in CopA-L/U/CopT-L/U.

Altogether these data indicate that removal of the bulged residues within the major stems of CopA and CopT resulted in a complex characterized by a fully base paired loop–loop helix whose formation was incompatible with subsequent formation of the stabilizer helix C.

A loop–loop interaction is insufficient to prevent ribosome binding

CopA-mediated inhibition works by steric interference: the CopA–CopT complex prevents binding of ribosomes at the *tap* translation initiation site (5). Even a truncated CopA, resembling CopI, inhibited RepA synthesis *in vivo*, although at somewhat reduced efficiency (32). CopI, although unable to form a stable complex with CopT, forms the four-way junction structure (8,13), and was capable of interfering transiently with ribosome binding *in vitro* (5). Since removal of the bulged residues inhibited the activity of the mutant antisense RNAs *in vivo* (21), we tested here whether the loop–loop interaction in the three mutant CopI–CopT complexes could interfere with ribosome binding.

Toeprinting analysis was used to monitor the formation of translation initiation complexes on mRNAs *in vitro* (33). Previous experiments showed that CopI-dependent inhibition of ribosome binding at the *tap* initiation site was only detectable after a short incubation time. Therefore, complexes between CopI and CopT carrying either mutation Lo, Up or L/U were pre-formed, at RNA concentrations allowing essentially quantitative formation of the kissing complex during pre-incubation. Thereafter, the ternary mRNA/30S/$tRNA_f^{Met}$ complex was formed by adding 30S subunits and $tRNA_f^{Met}$. Ternary complex formation was quantified over time by monitoring the signal of the *tap* toeprint (Fig. 5). For reference, the same experiments were carried out with the wild-type CopI/CopT and CopA/CopT complexes, respectively. As shown previously, inhibition by CopA is irreversible within the time interval assayed, whereas CopI-dependent inhibition was progressively lost with 50% inhibition after 2 min incubation (Fig. 5) (5). In contrast, the three homologous mutant CopI–CopT complexes were completely inactive in inhibition of initiation complex formation at the *tap* RBS (Fig. 5).

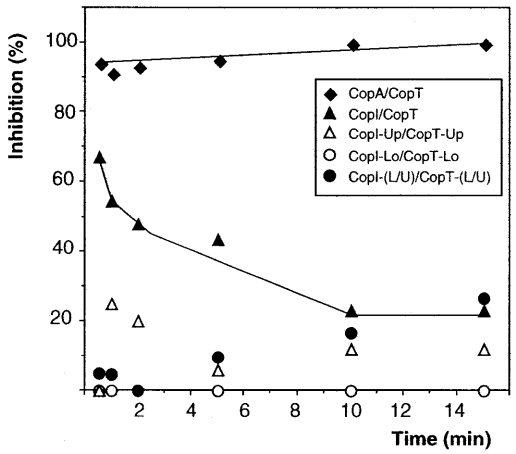

Figure 5. Kinetic analysis of antisense RNA-dependent inhibition of *tap* toeprints. Quantitations were done by Bioimager (BAS2000 Fuji) analysis of dried gels. Relative *tap* toeprint values were first calculated by relating the intensity of the toeprint to that of the run-off extension product. The yield of inhibition (%) was given by the signal of the relative *tap* toeprint in the presence of the antisense RNA divided by that of the relative toeprint in the absence of antisense RNA at a defined time. The different wild-type or mutated complexes are given in the insert. The values represent an average of three (wild-type) and two (mutant) independent experiments.

DISCUSSION

A common characteristic feature of most, if not all, prokaryotic antisense and target RNAs is the presence of well-defined stem–loop(s) as key structure elements. In many antisense regulatory systems, RNAs initiate binding by transient and reversible interactions between complementary loops and, depending on their particular topological constraints, use different pathways to proceed rapidly to more stable and inhibitory complexes (e.g. 9,11,34,35). Formation of sufficiently stable complexes is important to obtain maximal inhibition rates, and to achieve quasi-irreversible inhibition kinetics.

For CopA/CopT of plasmid R1, we have recently shown that the initial loop–loop interaction becomes disrupted when intermolecular base pairing is propagated into the upper stems, creating a four-way junction topology (Fig. 1C) (13). The same sequence of events is also supported for the truncated antisense RNA (CopI) which only contains the recognition stem–loop structure (Fig. 1). The four-way junction topology is essential to promote the formation of the additional intermolecular helix between the single-stranded regions of the two RNAs that results in the stable CopA–CopT complex (14). The question addressed here concerns the driving force for conversion of the initial loop–loop to the extended kissing complex. Both CopA and CopT carry, in the upper part of the recognition stem, several unpaired nucleotides. Replacement of these residues by Watson–Crick base pairs decreased binding rate *in vitro* and control *in vivo* (21). Given the magnitude of impairment, it could not be excluded that these mutant RNAs followed different binding pathways which did not initiate by a loop–loop interaction but instead by contacts within the 5′ single-stranded region of CopA. The experiments presented here indicate that removal of the bulged residues does not prevent the initial formation of a loop–loop helix, but abolishes the subsequent transition towards the four-way junction. Structure probing of the three homologous mutant RNA complexes indicates that helices B and B′ do not form (Figs 3 and 4). Instead, the data suggest that an intermolecular helix is formed between all 6 nucleotides in the complementary loop sequences, and that stem sequences do not participate in helix propagation. Interestingly, an extensively paired loop–loop helix was proposed for complexes between stem–loops of RNAI and RNAII of ColE1 (19,36). RNAI regulates ColE1 plasmid replication by inhibiting maturation of the pre-primer, RNAII. Binding is initiated by at least two loop–loop interactions followed by a series of reactions that progressively lead to the formation of a stable duplex (34,37). The NMR structures of two kissing complexes (6 and 7 bp loop–loop base pairs) have been solved (38–40). Both structures show full base pairing between the loops, and are characterized by a pronounced bend at the loop–loop helix towards the major groove. Interestingly, ethylation of any phosphate within the 6-nucleotide loop sequence of CopI-L/U prevents nucleation and initiation events for binding to CopT-L/U (Fig. 2). The dimerization of HIV-1 RNA which involves a loop–loop interaction between 6 complementary nucleotides in a 9-membered loop, is also inhibited by the ethylation of most of the phosphates of the loop nucleotides (29). However, in the wild-type CopA/CopT complex, where the initial interactions are transient, interference was restricted to the 5′ phosphates of the GCCA sequence of CopA and CopI, as well as to the complementary sequence of CopT. Weak interference observed at phosphates 114–120 of CopT implicates these residues in formation of helix B which is an early step required to commit the interacting RNAs to stable complex formation (14). Taken together, our study strongly argues for a striking difference in topology between complexes formed by the bulge-less mutant and wild-type RNAs.

In contrast to the ColE1 case where extensive loop–loop helices are involved in the inhibitory pathway, the loop–loop helix in the context of CopA-L/U/CopT-L/U is not productive since the long intermolecular stabilizer helix C cannot form (Fig. 3) (21). The suggested overall topology of the loop–loop helix tentatively explains this defect. Based on the known NMR loop–loop structures, a tertiary model for the CopA-L/U/CopT-L/U complex was built by graphic modeling, taking into account stereochemical constraints and probing data (Fig. 6). Despite the presence of a pronounced bend at the loop–loop helix, the two complementary regions that normally interact to give the stabilizer helix C are too far apart in space for efficient pairing (>100 Å; Fig. 6). In the ColE1 plasmid, the stem–loop structures of RNAI/II are shorter than in CopA/T, and bulged residues comparable to those in CopA/T are lacking (19). Also, bending at the loop–loop helix is further enhanced by Rom protein, most likely facilitating the distal contact between the 5′ tail of RNAI and its complement (38) which initiates full pairing. In plasmid R1 and related plasmids, no protein is known to play such a role. Instead, all these plasmids carry unpaired residues or bulged loops in the upper stem regions of antisense and target RNAs although their positions are not strictly conserved (15). These elements are essential for rapid *in vitro* binding and *in vivo* control [R1 (21); pMU720 (22); Col1b-P9 (23)]. In all these systems, the rapid conversion of the initial loop contacts to the extended kissing complexes is crucial for efficient inhibition. This step requires substantial melting of the upper stem regions of both antisense and target

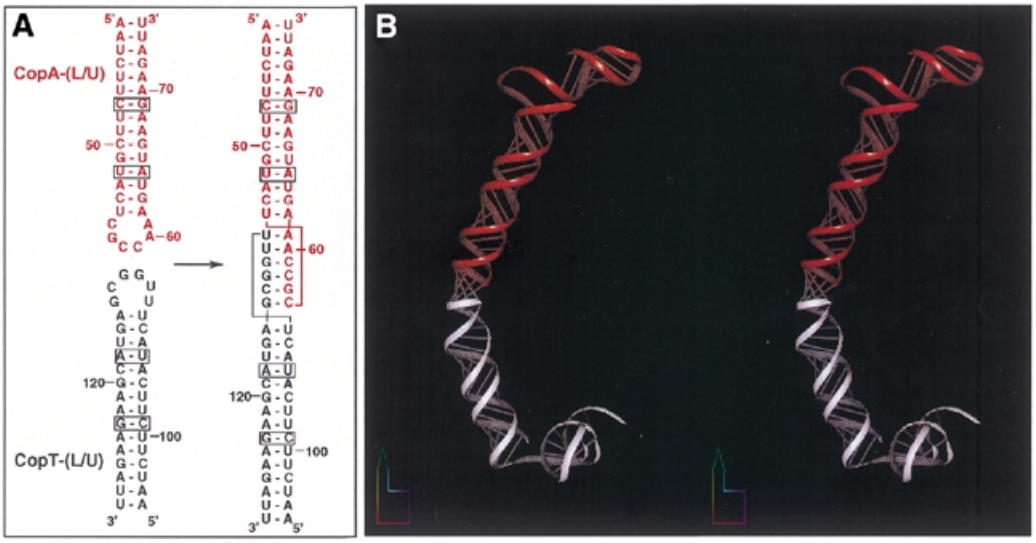

Figure 6. Models of the CopA-L/U/CopT-L/U complex. (**A**) Secondary structure representation and (**B**) stereoviews of the three-dimensional model of the CopA-L/U/CopT-L/U complex. Nucleotides in CopA-L/U [G1–U87] are shown in red, and in CopT-L/U [C88–A178] in white. The models were drawn with the program DRAWNA (28).

RNAs (9,11,13). We show here that, in the CopA/CopT system, this step is driven via the bulged residues; unpaired residues in the upper stems favor inter-strand helix progression over imperfect intra-strand base pairing. Bulged residues in long hairpin structures were also shown to be essential in other antisense regulated systems which initiate antisense/target binding via loop–linear RNA pairing (41–43).

Previous work showed that CopA inhibits the synthesis of RepA indirectly. Translation of a leader peptide, Tap, encoded immediately downstream of the CopA target site and in front of the *repA* reading frame is required for *repA* translation (4,44). CopA prevents ribosome binding at the *tap* ribosome loading site (5). Even CopI, although it only forms the four-way junction structure, transiently interferes with ribosome binding *in vitro* (Fig. 5) (5) and inhibits *repA* expression *in vivo* albeit at lower efficiency (32). Here we show that the CopI–CopT complexes carrying mutations Lo, Up and L/U do not inhibit ribosome binding at the *tap* RBS (Fig. 5). Since previous work has ruled out distal structure rearrangements in CopT as the mode of inhibition (12,13,45), the likely difference between inhibition (wild-type CopI–CopT) and lack of inhibition (bulge mutant CopI–CopT) should be due to their different structures. Even though CopI binds far upstream of the *tap* RBS, the bulky topology of the wild-type complex can sterically interfere with initiation, at least transiently. When full CopA is tested, the stabilizer helix C then renders inhibition irreversible. The suggested structure for the bulge mutant CopI–CopT complex (Fig. 6B) might be oriented so that ribosome access fails to be blocked. However, detailed structural analysis of the four-way junction topology will be required to elucidate the molecular mechanism by which a distal kissing complex can interfere with ribosome binding.

Intermolecular interactions between RNAs play fundamental roles in gene expression. Most of these are based on sequence complementarity, and loop–loop interactions are often implicated. *In vitro* selection approaches designed to select aptamers directed against RNA predominantly resulted in the isolation of sequences complementary to a hairpin loop in a defined structural context (46,47). It appears that, depending on the biological context of the RNA–RNA interaction, RNA structures have evolved either to 'freeze' a complex once formed or, alternatively, to convert initial interactions by propagating helices along topologically feasible pathways (reviewed in 48). In antisense regulation, formation of stable RNA–RNA complexes requires a propagation of the initial loop–loop helix to proceed rapidly to sufficiently stable and inhibitory complexes. The features that govern the high efficiency of natural antisense RNA are thus related to the secondary and tertiary structures of the interacting partners as well as of the complexes formed.

SUPPLEMENTARY MATERIAL

Coordinates of the molecular model of CopA-L/U/CopT-L/U complex are available as supplementary material at NAR Online.

ACKNOWLEDGEMENTS

We thank Hervé Moine for stimulating discussions and critical reading of the manuscript and G. Bec for advice. This work was supported by grants from the Centre National de la Recherche Scientifique (CNRS), and by the Swedish Natural Science Research Council (NFR, E.G.H.W.) and the Swedish Research Council for Engineering Sciences (TFR, E.G.H.W.).

REFERENCES

1. Wagner,E.G.H. and Simons,R.W. (1994) Antisense RNA control in bacteria, phages and plasmids. *Annu. Rev. Microbiol.*, **48**, 713–742.
2. Nordström,K., Molin,S. and Light,J. (1984) Control of replication of bacterial plasmids: genetics, molecular biology and physiology of the plasmid R1 system. *Plasmid*, **12**, 71–90.
3. Blomberg,P., Wagner,E.G.H. and Nordström,K. (1990) Control of replication of plamsid R1: the duplex between the antisense RNA, CopA and its target, CopT, is processed specifically *in vivo* and *in vitro* by RNase III. *EMBO J.*, **9**, 2331–2340.

4. Blomberg,P., Nordström,K. and Wagner,E.G.H. (1992) Replication control of plasmid R1: RepA synthesis is regulated by CopA RNA through inhibition of leader peptide translation. *EMBO J.*, **11**, 2675–2683.
5. Malmgren,C., Engdhal,H.M., Romby,P. and Wagner,E.G.H. (1996) An antisense/target RNA duplex or a strong intramolecular RNA structure 5′ of a translation initiation signal blocks ribosome binding: the case of plasmid R1. *RNA*, **2**, 1022–1032.
6. Wagner,E.G.H. and Brantl,S. (1998) Kissing and RNA stability in antisense control of plasmid replication. *Trends Biochem. Sci.*, **23**, 451–454.
7. Zeiler,B.N. and Simons,R.W. (1998) Antisense RNA structure and function. In Simons,R.W. and Grunberg-Manago,M. (eds), *RNA Structure and Function.* Cold Spring Harbor Laboratory Press, Cold Spring Harbor, NY, pp. 437–464.
8. Persson,C., Wagner,E. and Nordström,K. (1988) Control of replication of plasmid R1: kinetics of *in vitro* interaction between the antisense RNA, CopA and its target, CopT. *EMBO J.*, **7**, 3279–3288.
9. Siemering,K.R., Praszkier,J. and Pittard,A.J. (1994) Mechanism of binding of the antisense and target RNAs involved in the regulation of IncB plasmid replication. *J. Bacteriol.*, **176**, 2677–2688.
10. Asano,K., Niimi,T., Yokoyama,S. and Mizobuchi,K. (1998) Structural basis for binding of the plasmid ColIb-P9 antisense Inc RNA to its target RNA with the 5′-rUUGGCG-3′ motif in the loop sequence. *J. Biol. Chem.*, **273**, 11826–11838.
11. Asano,K. and Mizobuchi,K. (2000) Structural analysis of late intermediate complex formed between plasmid ColIb-P9 Inc RNA and its target RNA. How does a single antisense RNA repress translation of two genes at different rates? *J. Biol. Chem.*, **275**, 1269–1274.
12. Malmgren,C., Wagner,E.G.H., Ehresmann,C., Ehresmann,B. and Romby,P. (1997) Antisense RNA control of plasmid R1 replication. The dominant product of the antisense RNA-mRNA binding is not a full RNA duplex. *J. Biol. Chem.*, **272**, 12508–12512.
13. Kolb,F.A., Malmgren,C., Westhof,E., Ehresmann,C., Ehresmann,B., Wagner,E.G. and Romby,P. (2000) An unusual structure formed by antisense-target RNA binding involves an extended kissing complex with a four-way junction and a side-by-side helical alignment. *RNA*, **6**, 311–324.
14. Kolb,F.A., Engdahl,H.M., Slagter-Jager,J.G., Ehresmann,B., Ehresmann,C., Westhof,E., Wagner,E.G. and Romby,P. (2000) Progression of a loop–loop complex to a four-way junction is crucial for the activity of a regulatory antisense RNA. *EMBO J.*, **19**, 5905–5915.
15. Kolb,F.A., Westhof,E., Ehresmann,B., Ehresmann,C., Wagner,E.G.H. and Romby,P. (2001) Four-way junctions in antisense RNA-mRNA complexes involved in plasmid replication control: a common theme? *J. Mol. Biol.*, **309**, 605–614.
16. Wilson,I.W., Praszkier,J. and Pittard,A.J. (1993) Mutations affecting pseudoknot control of the replication of IncB group plasmids. *J. Bacteriol.*, **175**, 6476–6483.
17. Asano,K., Hama,C., Shin-ichi,I., Moriwaki,H. and Mizobuchi,K. (1999) The plasmid ColIb-P9 antisense Inc RNA controls expression of the RepZ replication protein and its positive regulator *repY* with different mechanisms. *J. Biol. Chem.*, **274**, 17924–17933.
18. Tomizawa,J. (1984) Control of ColE1 plasmid replication: the process of binding of RNAI and the primer transcript. *Cell*, **38**, 861–870.
19. Tomizawa,J. (1993) Evolution of functional structures of RNA. In Gesteland,R.F. and Atkins,J.F. (eds), *The RNA World*. Cold Spring Harbor Laboratory Press, Cold Spring Harbor, NY, pp. 419–445.
20. Hjalt,T.A. and Wagner,E.G.H. (1995) Bulged-out nucleotides protect an antisense RNA from RNase III cleavage. *Nucleic Acids Res.*, **23**, 571–579.
21. Hjalt,T.A. and Wagner,E.G. (1995) Bulged-out nucleotides in an antisense RNA are required for rapid target RNA binding *in vitro* and inhibition *in vivo*. *Nucleic Acids Res.*, **23**, 580–587.
22. Siemering,K.R., Praszkier,J. and Pittard,A.J. (1993) Interaction between the antisense and target RNAs involved in the regulation of IncB plasmid replication. *J. Bacteriol.*, **175**, 2895–2906.
23. Asano,K., Kato,A., Moriwaki,H., Hama,C., Shiba,K. and Mizobuchi,K. (1991) Positive and negative regulations of plasmid ColIb-P9 *repZ* gene expression at the translational level. *J. Biol. Chem.*, **266**, 3774–3781.
24. Maniatis,T., Fritsch,E.F. and Sambrook,J. (1982) *Molecular Cloning: A Laboratory Manual*. Cold Spring Harbor Laboratory Press, Cold Spring Harbor, NY.
25. Donis-Keller,H., Maxam,A. and Gilbert,W. (1977) Mapping adenines, guanines and pyrimidines in RNA. *Nucleic Acids Res.*, **4**, 2527–2538.
26. Westhof,E. (1993) Modeling the three-dimensional structure of ribonucleic acids. *J. Mol. Struct.*, **286**, 203–211.
27. Massire,C. and Westhof,E. (1998) MANIP: an interactive tool for modelling RNA. *J. Mol. Graph. Model*, **16**, 197–205, 255–257.
28. Massire,C., Gaspin,C. and Westhof,E. (1994) A program for drawing schematic views of nucleic acids. *J. Mol. Graph. Model*, **12**, 201–206.
29. Jossinet,F., Paillart,J.C., Westhof,E., Hermann,T., Skripkin,E., Lodmell,S.J., Ehresmann,C., Ehresmann,B. and Marquet,R. (1999) Dimerization of HIV-1 genomic RNA of subtypes A and B: RNA loop structure and magnesium binding. *RNA*, **5**, 1222–1234.
30. Givskov,M. and Molin,S. (1984) Copy mutants of plasmid R1: effects of base pair substitutions in the *copA* gene on the replication control system. *Mol. Gen. Genet.*, **194**, 286–292.
31. Chen,X., Woodson,S.A., Burrows,C.J. and Rokita,S.E. (1993) A highly sensitive probe for guanine N7 in folded structures of RNA: application to tRNA-Phe and Tetrahymena group I intron. *Biochemistry*, **32**, 7610–7616.
32. Wagner,E.G.H., Blomberg,P. and Nordström,K. (1992) Replication control in plasmid R1: duplex formation between the antisense RNA, CopA and its target, CopT, is not required for inhibition of RepA synthesis. *EMBO J.*, **11**, 1195–1203.
33. Hartz,D., McPheeters,D.S., Traut,R. and Gold,L. (1988) Extension inhibition analysis of translation initiation complexes. *Methods Enzymol.*, **164**, 419–425.
34. Tomizawa,J. (1990) Control of ColE1 plasmid replication: intermediates in the binding of RNAI and RNAII. *J. Mol. Biol.*, **212**, 683–694.
35. Persson,C., Wagner,E.G. and Nordstrom,K. (1990) Control of replication of plasmid R1: formation of an initial transient complex is rate-limiting for antisense RNA-target RNA pairing. *EMBO J.*, **9**, 3767–3775.
36. Eguchi,Y. and Tomizawa,J. (1991) Complexes formed by complementary RNA stem-loops: their formation, structures and interaction with ColE1 Rom protein. *J. Mol. Biol.*, **220**, 831–842.
37. Eguchi,Y. and Tomizawa,J. (1990) Complex formed by complementary RNA stem-loops and its stabilization by a protein: function of ColE1 Rom protein. *Cell*, **60**, 199–209.
38. Marino,J.P., Gregorian,R.S., Csankovszki,G. and Crothers,D.M. (1995) Bent helix formation between RNA hairpins with complementary loops. *Science*, **268**, 1448–1454.
39. Chang,K. and Tinoco,I.,Jr (1997) The structure of an RNA kissing hairpin complex of the HIV TAR hairpin loop and its complement. *J. Mol. Biol.*, **269**, 52–66.
40. Comolli,L.R., Pelton,J.G. and Tinoco,I.,Jr (1998) Mapping of a protein-RNA kissing hairpin interface: Rom and Tar-Tar*. *Nucleic Acids Res.*, **26**, 4688–5502.
41. Thisted,T., Sorensen,N.S., Wagner,E.G. and Gerdes,K. (1994) Mechanism of post-segregational killing: Sok antisense RNA interacts with Hok mRNA via its 5′-end single-stranded leader and competes with the 3′-end of Hok mRNA for binding to the mok translational initiation region. *EMBO J.*, **13**, 1960–1968.
42. Kittle,J.D., Simons,R.W., Lee,J. and Kleckner,N. (1989) Insertion sequence IS10 antisense pairing initiates by an interaction between the 5′ end of the target RNA and a loop in the antisense RNA. *J. Mol. Biol.*, **210**, 561–572.
43. Jain,C. (1995) IS10 antisense control *in vivo* is affected by mutations throughout the region of complementarity between the interacting RNAs. *J. Mol. Biol.*, **246**, 585–594.
44. Blomberg,P., Engdahl,H.M., Malmgren,C., Romby,P. and Wagner,E.G.H. (1994) Replication control of plasmid R1: disruption of an inhibitory RNA structure that sequesters the *repA* ribosome binding site permits tap-independent RepA synthesis. *Mol. Microbiol.*, **12**, 49–60.
45. Öhman,M. and Wagner,E.G.H. (1989) Secondary structure analysis of the RepA mRNA leader transcript involved in control of replication of plasmid R1. *Nucleic Acids Res.*, **17**, 2557–2579.
46. Scarabino,D., Crisari,A., Lorenzini,S., Williams,K. and Tochinni-Valentini,G.P. (1999) tRNA prefers to kiss. *EMBO J.*, **18**, 4571–4578.
47. Duconge,F., Di Primo,C. and Toulme,J. (2000) Is a closing "GA pair" a rule for stable loop–loop RNA complexes? *J. Biol. Chem.*, **275**, 21287–21294.
48. Grosjean,H., Houssier,C., Romby,P. and Marquet,R. (1998) Modulation role of modified nucleotides on RNA-RNA interaction. In Grosjean,H. and Benne,R. (eds), *Modification and Editing of RNA: The Alteration of RNA Structure and Function.* ASM press, WA, pp. 113–133.